THE EFFECT OF HYDRODYNAMIC INSTABILITIES ON THE PROPAGATION OF ENTROPY WAVES THROUGH NOZZLES AND ON THE GENERATION OF INDIRECT COMBUSTION NOISE

Ignacio Duran and Aimee Morgans

Imperial College of London

email: i.duran@imperial.ac.uk

Indirect noise is generated due to the acceleration of entropy waves through the turbine stages. Since these waves are mainly composed of density fluctuations, the acceleration is also unstable: any deformation of the wavefront is amplified by the Rayleigh Taylor instability. The initially perturbed entropy wave generates a vorticty field due to the acceleration which deforms the wave front. In this work we show that the growth rate of this instability is large compared to the residence time of the entropy wave in a typical aero-engine turbine.

1. Introduction

The generation of noise inside the combustion chamber is an issue for aero-engine manufacturers for two main reasons. On one hand, the noise generated propagates to the outlet of the engine contributing to the global aircraft noise. On the other hand, the noise generated by the flame is reflected in the turbine stages, generating acoustic modes, which further perturb the flame and generates in turn more noise. This feedback loop can become unstable, leading to a thermoacoustic instability as shown by Crocco and Cheng [1]. In typical aero-engines this undesired feedback usually limits the functional domain of the aero-engine to operating points with higher fuel consumption and pollutant emissions. The study of the noise generated by the flame is therefore a priority for the reduction of fuel consumption, pollutants and noise. The flame generates noise through two main mechanisms, as found by Marble and Candel [9]: the direct mechanism, in which the unsteady heat release generates acoustic waves, and the indirect mechanism, where the entropy waves (hot spots) generate noise when convected through the turbine blades. Leyko et al. [7] used a simple 1D model to show that the noise generated by the indirect mechanism can be up to an order of magnitude larger than the direct one. For this reason the study of entropy waves and their propagation is of great importance.

The study of combustion noise relies strongly on the propagation of both the acoustic and the entropy waves through non-homogeneous flows. This is of great importance for indirect noise in particular, where the acoustic waves are generated due to the acceleration of the entropy waves through the turbine stages. The first methods developed relied on the compact assumption (low-frequency) to provide the transfer functions of 1D nozzles [9] and 2D blade rows [2]. These methods have been extended recently for the non-compact case [10, 4, 14, 3, 5]. These low-order models assume in general that the entropy wave is only convected through the blade rows with a simple quasi-1D velocity.

This is generally not the case, since the entropy wave can be deformed due to the mean flow inhomogeneities, and is subject to hydrodynamic instabilities. The first mechanism was studied by Morgans et al. [11], showing that the wave was strongly deformed by the mean flow shear dispersion, but that global entropy levels remained constant. However, the deformation of the wave is expected to have an impact on the noise generated. The objective of this work is to study the second mechanism for the deformation of the entropy wave: hydrodynamic instabilities. These hydrodynamic instabilities are related to the Rayleigh Taylor mechanism [8, 15]: since the entropy wave is essentially a density gradient, its acceleration due to the mean flow is unstable and any perturbation of the wavefront will grow exponentially. Two differences arise with typical Rayleigh Taylor instability: first, in the usual case of a water-air interface under gravity, the density ratio is large $\mathcal{O}\left(10^3\right)$ while the acceleration term is weak (gravity). For typical entropy waves convected through turbine stages the density ratio is weak (typically 40K hot spots give an Atwood number $\mathcal{A} = \rho'/\rho \sim 10^{-1}$), while the acceleration term is several orders of magnitude larger than gravity (the ratio being $\mathcal{O}\left(10^5\right)$ for typical aero-engines). The second difference lies in the nature of the interface: while the typical Rayleigh Taylor instability assumes the interface to be infinitely thin, in an entropy wave the interface is of the order of O(2/λ), where λ is the wavelength of the waves. The thickness of this interface delays the growth of the Rayleigh Taylor instabilities developing in the wave front, as will be seen in section 2. This interface thickness is also time dependent: as the entropy wave is accelerated the wavelength increases as $\lambda = u/f$ where u is the mean axial velocity and f the frequency of the wave.

The rest of this article is organised as follows: in section 2, the effect of a finite-length interface on the traditional Rayleigh Taylor instability is studied. This is of great importance since entropy waves are generally low frequency, and therefore the density gradient is finite. In section 3 a simple model is derived to calculate the growth rate of the instability on the wave front. Numerical simulations are presented in 4 and conclusions are drawn in 5.

2. The effect of finite-length interface

In this section the effect of a finite-length interface on the Rayleigh-Taylor instability will be assessed. This will be done in an initially steady flow in which the external force driving the instability is gravity. The initial configuration is shown in figure 1(a): a heavy fluid is located on top of a lighter one. The interface between both can be characterised by a gradient with a characteristic length of $1/K$. In the case where this length tends to zero, the growth rate of any perturbation in the interface (of wavelength k) is given by the well known result of the Rayleigh Taylor instability,

$$(1) \qquad \alpha_{RT} = \sqrt{\frac{\rho_1 - \rho_2}{\rho_1 + \rho_2}ak}$$

where ρ_1 and ρ_2 are the heavy and light densities, a is the acceleration term and k is the wavelength of the initial perturbation.

This result is valid when the interface is infinitely thin (i.e. thin compared with the inverse of the wavelength of the perturbation k). When a finite-length interface is considered, the growth of the small scale perturbations is slowed. LeLevier et al. [6] developed an approach to obtain the growth rate of the Rayleigh Taylor instability for finite-length interfaces. They assumed an initial density field in the form,

$$(2) \qquad \rho_1 - \frac{1}{2}\delta \exp\left(-Ky\right) \quad y > 0$$

$$(3) \qquad \rho_2 + \frac{1}{2}\delta \exp\left(Ky\right) \quad y < 0$$

where $\delta = \rho_1 - \rho_2$ and K defines the gradient at the interface (of characteristic length $1/K$). Considering an initial perturbation of the interface in the form $cos(kx)$, and a velocity potential in the
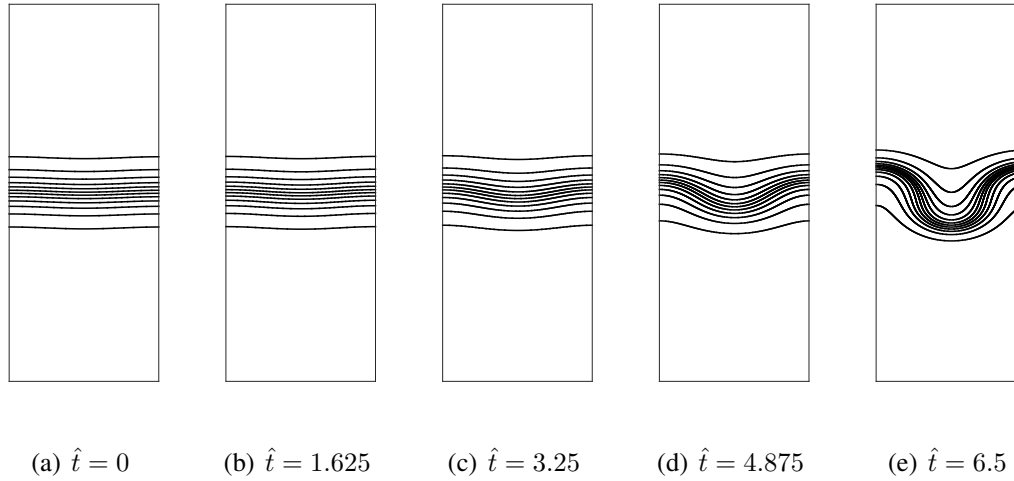
(a) $\hat{t} = 0$ (b) $\hat{t} = 1.625$ (c) $\hat{t} = 3.25$ (d) $\hat{t} = 4.875$ (e) $\hat{t} = 6.5$

Figure 1: Density isolines with $\hat{K} = 0.8$.

form

$$\phi = \exp\left(-Ky\right)cos(kx)f(t) \quad y > 0 \tag{4}$$

$$\phi = -\exp\left(Ky\right)cos(kx)f(t) \quad y < 0 \tag{5}$$

where f is the amplitude of the perturbation and is a function exclusively of time. LeLevier et al. [6] integrated the linearised Euler equations in the y direction in both the heavy and light fluids separately, and then applied matching conditions in the interface to obtain an expression for the function $f(t)$,

$$\frac{d^2 f}{dt^2} - a\frac{kK}{k+K}\frac{\delta}{\rho_1 + \rho_2}f = 0 \tag{6}$$

This leads to a growth rate

$$\alpha = \sqrt{\frac{a\delta}{\rho_1 + \rho_2}}\sqrt{\frac{kK}{k+K}} \tag{7}$$

which can be written as

$$\alpha = \alpha_{RT}\sqrt{\frac{\hat{K}}{1+\hat{K}}} \tag{8}$$

where $\hat{K} = K/k$ is the ratio between characteristic length of the perturbation and of the interface. The equation shows that the actual growth rate of a finite-length interface does not tend to infinity as the length scale of the perturbation tends to zero ($k \to \infty$), but is instead bounded by

$$\alpha_{max} = \sqrt{\frac{aK\delta}{\rho_1 + \rho_2}} \tag{9}$$

Using numerical simulations, the initial growth rate of perturbations was calculated for different values of $\hat{K}$. Figure 1 shows the evolution of the density isolines as a function of the dimensionless time, $\hat{t} = t\alpha_{RT}$, for the case $\hat{K} = 0.8$, computed using OpenFOAM [12]. Figure 2 plots the value of α/α_{RT} as a function of $\hat{K}$ for both numerical simulations and the analytical expression. (8).
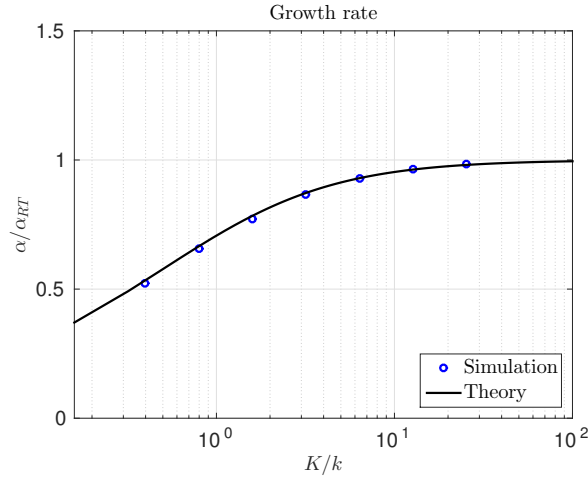
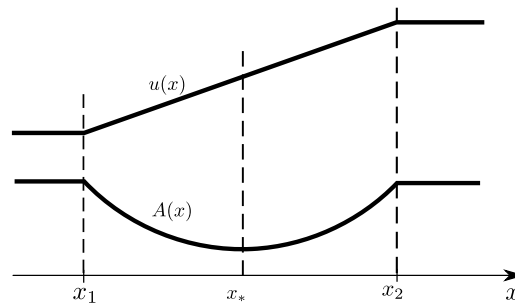Figure 2: Growth rate of the hydrodynamic instability as a function of $\hat{K}$.

Figure 3: Linear mean velocity profile nozzle. $A(x)$ is the cross-section area and $u(x)$ the velocity.

3. The acceleration of entropy waves

An entropy wave is a hydrodynamic perturbation composed mainly of temperature (or density) fluctuations. The order of magnitude of the entropy wave is related to the density and temperature fluctuations by

$$(10) \qquad \mathcal{O}\left(\frac{s'}{c_p}\right) \sim \mathcal{O}\left(\frac{\rho'}{\rho}\right) \sim \mathcal{O}\left(\frac{T'}{T}\right)$$

This hydrodynamic wave generates acoustic waves when accelerated with the mean flow, as explained in Marble and Candel [9]. When this occurs, the density fluctuations are subject to a Rayleigh Taylor instability in which the acceleration term is due to the mean pressure gradient ($a = -\nabla p/\rho$) which, for a steady quasi-one-dimensional nozzle flow, is equal to

$$(11) \qquad a = u\frac{du}{dx}.$$

Lets assume for simplicity a linear mean velocity nozzle as done in the second part of Marble and Candel [9] (see figure 3). In such case, the nozzle extends between x_1 and x_2, and the velocity profile is given by $u(x)/c_* = x/x_*$, where x_* and c_* denote the axial coordinate and the speed of sound at the nozzle throat respectively. Under such assumption, the acceleration term is linear in x,

$$(12) \qquad a = \frac{c_*^2}{x_*}\frac{x}{x_*}.$$

Since the flow is accelerating, the wavelength (λ) of the perturbation increases with the x coordinate. This gives,

$$(13) \qquad K \sim \frac{2}{\lambda} \sim \frac{2f}{u(x)} \sim \frac{2f}{c_*\left(x/x_*\right)}.$$
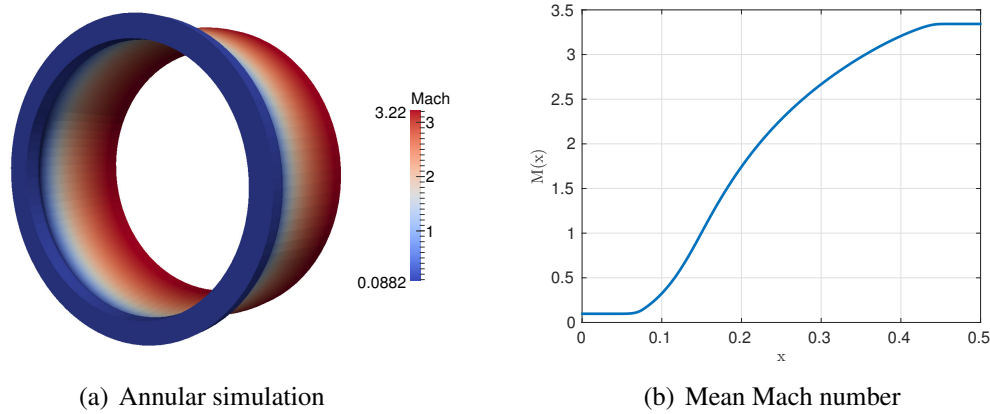
(a) Annular simulation

(b) Mean Mach number

Figure 4: Geometry of the numerical simulations

$$(14) \qquad \alpha(x) \sim \left[\frac{c_* f}{x_*} \frac{\rho'}{\rho} \frac{k}{k+K} \right]^{1/2}$$

As an order of magnitude, lets consider a temperature fluctuation of $T' \sim 40$K in an aero-engine in which $T \sim 800$ and with inlet and outlet Mach numbers of $M_1 = 0.1$ and $M_2 = 3$. The density fluctuations are then $\rho'/\rho \sim 0.05$, the speed of sound at the throat $c_* \sim 550$m/s and the characteristic length of the throat can be taken to be $x_* \sim 0.1$m. Assuming a frequency of 500Hz, typical of combustion noise, the initial growth rate of the instability, given by equation (8) is $\alpha \sim 200 s^{-1}$. This means that the characteristic time of the instability would be $\tau_I \sim 5 \cdot 10^{-3}$s, while the convective time of the entropy wave (the time that it takes for the entropy wave to accelerate from M_1 to M_2 in such a nozzle) is $\tau_C \sim 5 \cdot 10^{-4}$s. The ratio of both $\tau_I/\tau_C \sim \mathcal{O}(10)$ shows that the effect of the Rayleigh Taylor instability in such a configuration can have some effect, though the time it takes to develop is of the order of 10 times larger than the residence time. However, when considering higher frequencies and larger amplitudes, the ratio decreases. As seen from equation (8), this type of hydrodynamic instability has little or no effect on low frequency combustion noise, but may be important for higher frequency entropy waves, which are deformed by this mechanism.

4. Numerical simulations

Numerical simulations are now performed using the code OpenFOAM [12]. The configuration is shown in figure 4: an annular nozzle with inlet/outlet Mach numbers of 0.1 and 3.2 respectively is simulated. The mesh contains 500 cells in the x-direction, 88 in the θ-direction and one in the radial direction. This has been found sufficient to reduce numerical dissipation.

Using NSCBC [13] boundary conditions, an entropy wave is introduced in the simulation domain through the inlet. The forcing term is a plane sinusoidal wave of $f = 500$Hz and an amplitude of $s'/c_p = 0.05$, with a small azimuthal perturbation in the form of a time delay, with a maximum value of 25% of the period of the wave. Figure 4 show the entropy wave propagating through the domain. While convected, the deformed wave is subject to the Rayleigh Taylor instability mechanism, generating a vorticity field (shown in figure 4 as contour lines). This vorticity is convected with the mean flow and contributes to the deformation of the wavefront.

5. Conclusions

The generation of indirect noise is due to the acceleration of hot spots (entropy waves) through turbine stages. This acceleration is affected by the Rayleigh Taylor instability since the entropy wave

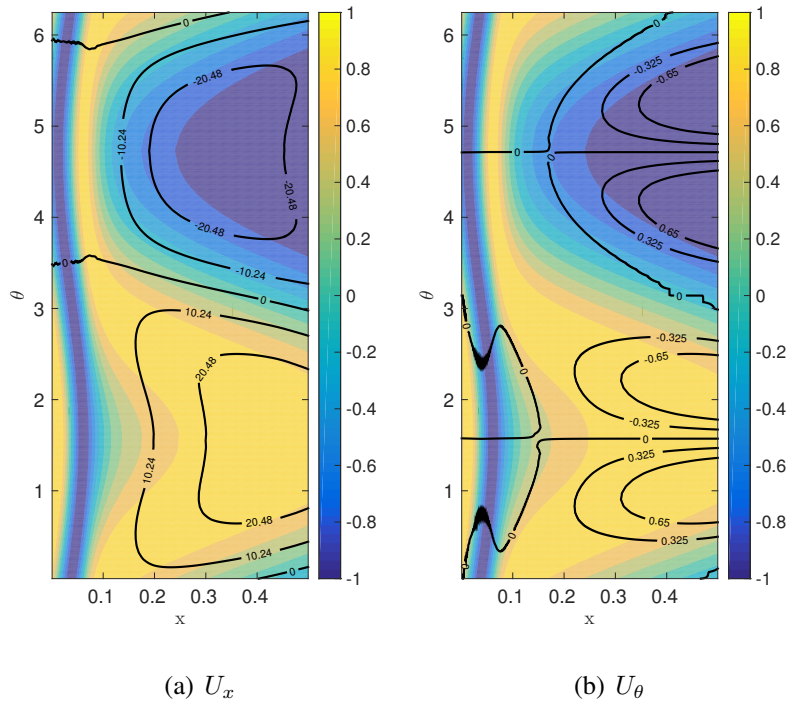(a) U_x (b) U_θ

Figure 5: Plot of the entropy wave propagating through the nozzle. Contour lines of the induced velocity.

is composed of a density perturbation. In this work we have shown that the growth rate is, as a first approximation, proportional to the square root of the frequency, meaning that for low frequencies the effect is likely to be negligible since the instability does not have time to develop. However, at higher frequencies ($1000 - 2000$Hz) the characteristic time for the growth of the instability is comparable to the residence time of the entropy wave in the nozzle, showing that the wave can be deformed strongly and therefore generate less indirect noise. Numerical simulations confirm that the deformed entropy wave generates a vorticity field that deforms the wavefront.

REFERENCES

1. L. Crocco and S. I. Cheng. *Theory of combustion instability in liquid propellant rocket motors*. Number Agardograph No 8. Butterworths Science, 1956.

2. N. A. Cumpsty and F. E. Marble. The interaction of entropy fluctuations with turbine blade rows; a mechanism of turbojet engine noise. *Proc. R. Soc. Lond. A* , 357:323–344, 1977.

3. I. Duran and S. Moreau. Solution of the quasi one-dimensional linearized Euler equations using flow invariants and the Magnus expansion. *Journal of Fluid Mechanics*, 723:190–231, May 2013.

4. A. Giauque, M. Huet, and F. Clero. Analytical Analysis of Indirect Combustion Noise in Sub-critical Nozzles. *J. Eng. Gas Turbines Power*, 134(11):111202, 2012.

5. I. Duran and A. Morgans. On the reflection and transmission of circumferential waves through nozzles. *Journal of Fluid Mechanics*, Under Review, 2015.

6. R. LeLevier, G. Lasher, and F. Bjorklund. Effect of a density gradient on Taylor instability. (UCRL-4459), 1955.

7. M. Leyko, F. Nicoud, and T. Poinsot. Comparison of direct and indirect combustion noise mechanisms in a model combustor. *AIAA Journal*, 47(11):2709–2716, 2009.

8. Lord Rayleigh. Investigation of the character of the equilibrium of an incompressible heavy fluid of variable density. *Proceedings of the London Mathematical Society*, 14: 170-177, 1883.

9. F. E. Marble and S. Candel. Acoustic disturbances from gas nonuniformities convected through a nozzle. *J. Sound Vib.*, 55:225–243, 1977.

10. W. H. Moase, M. J. Brear, and C. Manzie. The forced response of choked nozzles and supersonic diffusers. *Journal of Fluid Mechanics*, 585:281–304, 2007.

11. A. S. Morgans, C. S. Goh, and J. A. Dahan. The dissipation and shear dispersion of entropy waves in combustor thermoacoustics. *Journal of Fluid Mechanics*, 733 R2:1–11, 2013.

12. OpenFOAM. http://www.openfoam.org.

13. T. Poinsot, T. Echekki, and M. G. Mungal. A study of the laminar flame tip and implications for premixed turbulent combustion. *Combust. Sci. Tech.*, 81(1-3):45–73, 1992.

14. S. R. Stow, A. P. Dowling, and T. P. Hynes. Reflection of circumferential modes in a choked nozzle. *Journal of Fluid Mechanics*, 467:215–239, 2002.

15. Taylor, Sir Geoffrey Ingram . The instability of liquid surfaces when accelerated in a direction perpendicular to their planes. *Proceedings of the Royal Society of London. Series A, Mathematical and Physical Sciences*, 201 (1065): 192-196, 1950.